

## Superexpanded Prussian-Blue Analogue with $[\text{Fe}(\text{CN})_6]^{4-}$ , $[\text{Nb}_6\text{Cl}_{12}(\text{CN})_6]^{4-}$ , and $[\text{Mn}(\text{salen})]^+$ as Building Units

Jianjun Zhang and Abdessadek Lachgar\*

Department of Chemistry, Wake Forest University, Winston-Salem, North Carolina 27109

Received August 28, 2006; E-mail: lachgar@wfu.edu

The rational design and development of synthetic methodologies toward the assembly of complex crystalline solids with topologies that can to a certain extent be predicted from the structure of the molecular building blocks has achieved tremendous success in different fields of materials chemistry.<sup>1,2</sup> The approach has been widely applied to the assembly of cyano-bridged materials with diverse structural and physical properties.<sup>3</sup> These systems consist of networks built of polycyanometallate and simple metal ions or coordinatively unsaturated complexes connected by CN ligands. Among these compounds, the most widely investigated are Prussian blue and its analogues, which constitute a family of complex-based magnetic materials with properties that can be affected through the judicious choice of the building blocks components. Octahedral metal clusters are being investigated as building blocks for a variety of frameworks owing to their large size (~1 nm) and remarkable physical properties that arise from the presence of metal–metal bonds.<sup>4,5</sup> The replacement of  $[\text{Fe}(\text{CN})_6]^{4-}$  by octahedral cluster analogues  $[\text{Re}_6\text{X}_8(\text{CN})_6]^{n-}$  (X = chalcide) or  $[\text{Nb}_6\text{X}_{12}(\text{CN})_6]^{n-}$  (X = Cl, Br) has led to the preparation of expanded Prussian-blue-type frameworks with large cavities and sometimes interesting gas absorption properties.<sup>6</sup>

In the search for new magnetic materials, several attempts have been made to synthesize compounds with extended structures containing three different spin centers.<sup>7</sup> Interesting cluster–metal ion magnetic interactions have also been observed in a cluster-based 0D heterotrimetallic compound.<sup>8</sup> We have previously reported the Prussian-blue analogue  $[\text{Me}_4\text{N}]_2[\text{Mn}(\text{Nb}_6\text{Cl}_{12}(\text{CN})_6)]$  built of  $[\text{Nb}_6\text{Cl}_{12}(\text{CN})_6]^{4-}$  and Mn(II) ions connected via CN ligands.<sup>6a</sup> Furthermore, reaction between Mn(III) complexes with salen-type tetradentate Schiff-base ligands and  $[\text{Nb}_6\text{Cl}_{12}(\text{CN})_6]^{4-}$  resulted in the assembly of different types of supramolecular species.<sup>9</sup> Here we report the synthesis and properties of a trimetallic compound:  $[\text{H}_3\text{O}]_2[\text{Fe}(\text{CN})_6(\text{Mn}(\text{salen}))_6\text{Nb}_6\text{Cl}_{12}(\text{CN})_6] \cdot 3\text{H}_2\text{O}$  (**1**) which incorporates  $[\text{Fe}(\text{CN})_6]^{4-}$ ,  $[\text{Nb}_6\text{Cl}_{12}(\text{CN})_6]^{4-}$ , and  $[\text{Mn}(\text{salen})]^+$  as building units linked via cyanide ligands to form a 3D framework that can be described as a superexpanded Prussian-blue analogue. The compound represents the first successful attempt to incorporate mononuclear cyanometallate complexes and cyano-substituted octahedral metal clusters into the same framework.

A one-pot reaction between  $[\text{Et}_4\text{N}]_3[\text{Fe}(\text{CN})_6]$ ,  $[\text{Mn}(\text{salen})\text{Cl}(\text{H}_2\text{O})]$ , and  $(\text{Me}_4\text{N})_4[\text{Nb}_6\text{Cl}_{12}(\text{CN})_6]$  in water/methanol led to the precipitation of **1** as microcrystalline powder.<sup>10</sup> Crystals suitable for single-crystal XRD analysis were grown by the layering method.

The structure of **1** consists of a 3D anionic framework  $[\text{Fe}(\text{CN})_6(\text{Mn}(\text{salen}))_6\text{Nb}_6\text{Cl}_{12}(\text{CN})_6]^{2-}$  built of  $[\text{Fe}(\text{CN})_6]^{4-}$  and  $[\text{Nb}_6\text{Cl}_{12}(\text{CN})_6]^{4-}$  nodes connected by  $[\text{Mn}(\text{salen})]^+$  complexes via (Fe–C≡N–Mn–N≡C–Nb) coordination bonds (Figure 1a).<sup>11</sup> Each node coordinates to six  $[\text{Mn}(\text{salen})]^+$  complexes through CN ligands. The structure of  $[\text{Nb}_6\text{Cl}_{12}(\text{CN})_6]^{4-}$  is the same as that observed in the cluster precursor and in other previously reported compounds containing this cluster as building unit.<sup>6a,9</sup> The mean

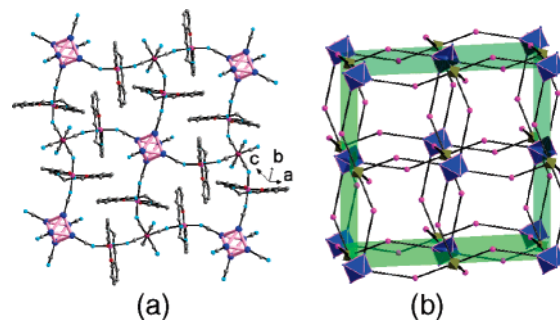


**Figure 1.** (a) A projection of the overall structure of **1**; (b) a schematic diagram showing the pseudocubic lattice and the connectivity between  $[\text{Fe}(\text{CN})_6]^{4-}$  and  $[\text{Nb}_6\text{Cl}_{12}(\text{CN})_6]^{4-}$  nodes through  $[\text{Mn}(\text{Salen})]^+$ . Hydronium ions and water molecules located in the cavities have been omitted.

Nb–Nb (2.9401(7)) and Nb–Cl (2.4640(11) Å) are consistent with 16 valence electrons available for metal–metal bonding. The Nb–C (2.275(5) Å) and C≡N (1.151(6) Å) are similar to those observed in other compounds containing octahedral cyanochloride niobium clusters. For the  $[\text{Fe}(\text{CN})_6]^{4-}$  node, the mean Fe–C bond length (1.939(5) Å) is similar to those observed in other compounds containing  $[\text{Fe}(\text{CN})_6]^{4-}$  (Fe–C, 1.916(3)–1.968(5) Å).<sup>12,13</sup> The mean C≡N bond length and Fe–C≡N angle are 1.150(6) Å and 176.3(5)°, respectively. The IR spectrum shows two bands in the 2200–2000  $\text{cm}^{-1}$  region. The first band at 2121  $\text{cm}^{-1}$  is characteristic of the bridging CN ligand in the  $16e^- \{ \text{Nb}_6 \}$  cluster. The second band at 2045  $\text{cm}^{-1}$  corresponds to the stretching mode of the bridging CN attached to Fe(II).<sup>13,14</sup> Reduction of Fe<sup>III</sup> to Fe<sup>II</sup> is probably due to the protic solvents.<sup>13,14</sup>

The Mn(III) ion is chelated by the tetradentate salen ligand and uses its two remaining axial coordination sites to link to two cyanide ligands from  $[\text{Fe}(\text{CN})_6]^{4-}$  and  $[\text{Nb}_6\text{Cl}_{12}(\text{CN})_6]^{4-}$  nodes, respectively. The mean Mn–N (CN–Nb) bond length (2.314(4) Å) is smaller than that of the Mn–N (CN–Fe) (2.343(4) Å), reflecting the Jahn–Teller effect of Mn(III) ions. Each  $[\text{Mn}(\text{salen})]^+$  group coordinates to the two different nodes in *cis*-mode with an Fe–Mn–Nb angle of 135.728(2)°.

The 3D structure of **1** (Figure 1b) can be viewed as a distorted cubic face centered framework that consists of identical but staggered 2D diamondoid net in which the nodes  $[\text{Nb}_6\text{Cl}_{12}(\text{CN})_6]^{4-}$  and  $[\text{Fe}(\text{CN})_6]^{4-}$  are connected through four cyanide ligands to four different  $[\text{Mn}(\text{salen})]^+$ . Each node uses its remaining CN ligands to connect the layers via  $[\text{Mn}(\text{salen})]^+$  units to form a 3D framework that can be considered as superexpanded Prussian-blue analogue built of two different hexacyano building units and expanded by the insertion of  $[\text{Mn}(\text{salen})]^+$  complex. In Prussian blue and its cluster analogue, the cyano-nodes are 75% occupied leading to neutral 3D framework,<sup>6</sup> while in **1** the  $[\text{Fe}(\text{CN})_6]^{4-}$  and  $[\text{Nb}_6\text{Cl}_{12}(\text{CN})_6]^{4-}$  sites are fully occupied leading to anionic framework.

No  $[\text{NMe}_4]^+$  or  $[\text{NEt}_4]^+$  ions were found in the cavities, only oxygen atoms of disordered water and hydronium ions could be

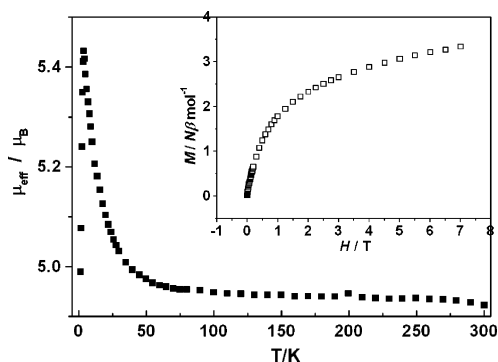


**Figure 2.** Temperature dependence of the effective magnetic moment  $\mu_{\text{eff}}$  of **1** and field dependence of magnetization at 1.8 K (insert).

located in the electron density map. The number of  $\text{H}_2\text{O}^+$  was determined from charge balance while the presence of three water molecules per molecular formula was confirmed by thermogravimetric analysis (TGA) which shows that **1** loses all  $\text{H}_2\text{O}$  reversibly before 120 °C (exptl, 2.67%; calcd, 2.67%) and simultaneous proton transfer to the framework. The compound continues to lose weight in a broad step and begins to form a stable phase after 680 °C. The final product at 950 °C was determined by powder X-ray diffraction (PXRD) to be a mixture of  $\text{Mn}_4\text{Nb}_2\text{O}_9$  and  $\text{MnNb}_2\text{O}_6$  ( $M = \text{Mn}, \text{Fe}$ ). The effective free volume in **1** is about 14.0% of the unit cell volume, as calculated by the program PLATON.<sup>15</sup> This value is almost twice that of  $[\text{Na}[\text{Mn}(\text{salen})_3][\text{Re}_6\text{Se}_8(\text{CN})_6]$ , 7.8%).<sup>6c</sup> The  $\text{N}_2$  sorption isotherms were measured and revealed reversible type II isotherms. The surface area of **1** was determined to be 55.4  $\text{m}^2/\text{g}$  (BET model), compared with 38, 46.7, and 500  $\text{m}^2/\text{g}$  for  $\text{Fe}_4[\text{Fe}(\text{CN})_6]_3$ ,  $\text{Ga}[\text{Re}_6\text{Se}_8(\text{CN})_6]$ , and Faujasite, respectively.<sup>6f,16</sup>

The electron spin resonance (ESR) spectrum of **1** measured on microcrystalline sample at room temperature shows a broad peak with  $g = 1.986$  which can be attributed to the 16e cluster unit. The ESR data of the polycrystalline and methanol solution of 16e cluster  $[\text{Nb}_6\text{Cl}_{12}(\text{CN})_6]^{4-}$  also exhibit the same signal that may be attributed to the large temperature-independent paramagnetism of the cluster.<sup>17</sup> Magnetic susceptibility ( $\chi_M$ ) data for **1** were measured from 300 to 1.8 K at an applied field of 2 T (Figure 2). At 300 K,  $\mu_{\text{eff}} = 4.92 \mu_B$  indicates the presence of high-spin Mn(III) ( $4.89 \mu_B$  for  $S = 2$ ). As the system is cooled,  $\mu_{\text{eff}}$  smoothly increases from 300 to 50 K and then abruptly increases to reach a maximum  $5.43 \mu_B$  at 3.5 K. Below 3.5 K,  $\mu_{\text{eff}}$  sharply decreases to reach  $4.98 \mu_B$  at 1.8 K, most likely due to zero-field splitting (ZFS) of anisotropic high-spin  $\text{Mn}^{3+}$  ions. The  $\chi_M^{-1}$  versus  $T$  plot follows the Curie–Weiss law with the Weiss constant  $\theta = 1.16$  K. The positive  $\theta$  value and increase of  $\mu_{\text{eff}}$  over the entire temperature range indicates ferromagnetic coupling. In variable-field measurements, the magnetization sharply increases to  $\sim 2.33 N\beta \text{ mol}^{-1}$  at fields weaker than 2 T, then gradually increases to  $3.33 N\beta \text{ mol}^{-1}$  at 7 T, not reaching the saturation state of  $g\Sigma s = 4N\beta \text{ mol}^{-1}$ , which may be because a larger magnetic field is required to reach saturation owing to the ZFS of high-spin Mn(III). In the AC magnetic susceptibility measurements the out-of-phase magnetization shows a sharp increase as the system is cooled. The origin and the type of magnetic ordering in this system is not yet completely understood and further experiments are needed; however, electronic communication via the diamagnetic  $[\text{Fe}(\text{CN})_6]^{4-}$  building block has been previously

reported.<sup>12a,13,18</sup> Magnetic interactions can also be mediated by electrostatic interactions between salen ligands. Indeed the closest contact between ligands is found to be  $H_{\text{BB}}\text{-ring} = 2.63 \text{ \AA}$  indicating relatively strong edge-to-face  $\pi\text{-}\pi$  interactions.

**Acknowledgment.** This material is based upon work supported by the National Science Foundation under Grant Nos. DMR-0446763 and 0234489.

**Supporting Information Available:** X-ray crystallographic data in CIF format; bond lengths and angles; detailed synthesis process and other supplementary figures. This material is available free of charge via the Internet at <http://pubs.acs.org>.

## References

- (1) Robson, R.; Abrahams, B. F.; Batten, S. R.; Gable, R. W.; Hoskins, B. F.; Liu, J. *Supramolecular Architecture*; ACS: Washington, DC, 1992; Chapter 19.
- (2) (a) Holliday, B. J.; Mirkin, C. A. *Angew. Chem., Int. Ed.* **2001**, *40*, 2022. (b) Yaghi, O. M.; Li, H. L.; Davis, C.; Richardson, D.; Groy, T. L. *Acc. Chem. Res.* **1998**, *31*, 474 and references therein.
- (3) Selected reviews: (a) Sieklucka, B.; Podgajny, R.; Przychodzen, P.; Korzeniak, T. *Coord. Chem. Rev.* **2005**, *249*, 2203. (b) Beltran, L. M. C.; Long, J. R. *Acc. Chem. Res.* **2005**, *38*, 325. (c) Miller, J. S.; Manson, J. L. *Acc. Chem. Res.* **2001**, *34*, 563. (d) Dunbar, K. R.; Heintz, R. A. *Prog. Inorg. Chem.* **1997**, *45*, 283.
- (4) Selected reviews: (a) Welch, E. J.; Long, J. R. *Prog. Inorg. Chem.* **2005**, *54*, 1. (b) Gabriel, J.-C. P.; Boubekeur, K.; Uriel, S.; Batail, P. *Chem. Rev.* **2001**, *101*, 2037. (c) Selby, H. T.; Roland, B. K.; Zheng, Z. P. *Acc. Chem. Res.* **2003**, *36*, 933. (d) Gray, T. G. *Coord. Chem. Rev.* **2003**, *243*, 213.
- (5) Some cluster-cyanide based frameworks: (a) Jin, S.; DiSalvo, F. J. *Chem. Mater.* **2002**, *14*, 3448. (b) Bennett, M. V.; Shores, M. P.; Beauvais, L. G.; Long, J. R. *J. Am. Chem. Soc.* **2000**, *122*, 6664.
- (6) 3D Prussian-blue analogues: (a) Yan, B. B.; Zhou, H. J.; Lachgar, A. *Inorg. Chem.* **2003**, *42*, 8818. (b) Naumov, N. G.; Soldatov, D. V.; Ripmeester, J. A.; Artemkina, S. B.; Federov, V. E. *Chem. Commun.* **2001**, 571. (c) Beauvais, L. G.; Shores, M. P.; Long, J. R. *J. Am. Chem. Soc.* **2000**, *122*, 2763. (d) Shores, M. P.; Beauvais, L. G.; Long, J. R. *Inorg. Chem.* **1999**, *38*, 1648. (e) Kim, Y.; Park, S. M.; Kim, S. J. *Inorg. Chem. Commun.* **2002**, *5*, 592. (f) Bennett, M. V.; Beauvais, L. G.; Shores, M. P.; Long, J. R. *J. Am. Chem. Soc.* **2001**, *123*, 8022. (g) Naumov, N. G.; Cordier, S.; Perrin, C. *Solid State Sci.* **2005**, *7*, 1517. (h) Beauvais, L. G.; Long, J. R. *Inorg. Chem.* **2006**, *45*, 236.
- (7) (a) Kou, H. Z.; Zhou, B. C.; Gao, S.; Wang, R. J. *Angew. Chem., Int. Ed.* **2003**, *42*, 3288. (b) Gheorghe, R.; Andruh, M.; Costes, J. P.; Donnadieu, B. *Chem. Commun.* **2003**, 2778. (c) Berlinguette, C. P.; Dunbar, K. R. *Chem. Commun.* **2005**, 2451.
- (8) Tulskey, E. G.; Crawford, N. R. M.; Baudron, S. A.; Batail, P.; Long, J. R. *J. Am. Chem. Soc.* **2003**, *125*, 15543.
- (9) (a) Zhou, H.; Day, C. S.; Lachgar, A. *Chem. Mater.* **2004**, *16*, 4870. (b) Zhou, H.; Day, C. S.; Lachgar, A. *Cryst. Growth Des.* **2006**, *6*, 2384. (c) Zhou, H.; Cloix, B.; Strates, T.; Munoz, M.; Lachgar, A. *Chem. Mater.*, to be submitted for publication, 2006.
- (10) The identity of the product was checked by comparing its powder XRD to that calculated based on the crystal structure determined from single-crystal XRD (Supporting Information).
- (11) Crystal data for **1**:  $\text{C}_{108}\text{H}_{95}\text{Cl}_{12}\text{FeMn}_6\text{N}_{24}\text{Nb}_6\text{O}_{17}$ , rhombohedral, R-3,  $a = 16.3466(18)$ ,  $b = 42.227(9)$  Å,  $V = 9772(3)$  Å<sup>3</sup>,  $Z = 3$ ,  $R_1$  [4103 observed reflections with  $I > 2\sigma(I)$ ] = 0.0528,  $wR_2 = 0.1282$  (all data), GOF = 1.102 (269 parameters).
- (12) (a) Mondal, N.; Saha, M. K.; Bag, B.; Mitra, S.; Gramlich, V.; Ribas, J.; Fallah, M. S. E. *J. Chem. Soc., Dalton Trans.* **2000**, 1601. (b) Zhang, H. X.; Tong, Y. X.; Chen, Z. N.; Yu, K. B.; Kang, B. S. *J. Organomet. Chem.* **2000**, *598*, 63.
- (13) (a) Thetiot, F.; Triki, S.; Pala, J. S. *New J. Chem.* **2002**, *26*, 196. (b) Hong, C. S.; You, Y. S. *Inorg. Chim. Acta* **2004**, *357*, 3271.
- (14) (a) Lopez, J. P.; Heinemann, F. W.; Grohmann, A. Z. *Anorg. Allg. Chem.* **2003**, *629*, 2449. (b) Parker, R. J.; Piccia, L.; Moubaraki, B.; Murray, K. S.; Hockless, D. C. R.; Rae, A. D.; Willis, A. C. *Inorg. Chem.* **2002**, *41*, 2489.
- (15) Spek, A. L. *PLATON*, version 1.62; University of Utrecht, Utrecht, The Netherlands, 1999.
- (16) Breck, D. W. *Zeolite Molecular Sieves*; Wiley & Sons: New York, 1974.
- (17) (a) Mackay, R. A.; Schneider, R. F. *Inorg. Chem.* **1967**, *6*, 549. (b) Converse, J. G.; McCarty, R. E. *Inorg. Chem.* **1970**, *9*, 1361.
- (18) Fukita, N.; Ohba, M.; Okawa, H.; Matsuda, K.; Iwamura, H. *Inorg. Chem.* **1998**, *37*, 842.

JA066104C